A Novel Robust Detection Algorithm for Spectrum Sensing

Lu Lu, Hsiao-Chun Wu, *Senior Member, IEEE,* and S. S. Iyengar, *Fellow, IEEE*

***Abstract*—In this paper, the DTV (digital television) spectrum sensing problem is studied, which plays a key role in the cognitive radio. In contrast to the existing higher-order-statistics (HOS) approach, we propose a novel robust spectrum-sensing method, which is based on the JB (Jarqur-Bera) statistic. In our studies, the existing detector may often not be robust when the sample size is small. Our proposed JB detector is heuristically justified to be superior for the simulated microphone signals as well as the real DTV signals. Moreover, the computational complexity analysis for our proposed new JB detector and the HOS detector is also presented. Ultimately, the normality test and the spectral analysis are provided to justify the advantage of our proposed spectrum sensing method.**

***Index Terms*—Spectrum sensing, signal detection, higher-order-statistics (HOS), JB (Jarqur-Bera) statistic, DTV.**

I. Introduction

THERE always exists the need for the communication services at higher data rates. Given the limitation of the natural frequency spectrum, it becomes obvious that the current static frequency allocation schemes can not accommodate the users' requirement on the high data rates. As a result, innovative techniques that can offer new ways of exploiting the available spectrum are needed. The increasing demand for wireless connectivity and the crowded unlicensed spectra have prompted the regulatory agencies to be more aggressive in coming up with new ways to use spectra more wisely [1]. Hence, cognitive radio (see [2], [3]) arises as a feasible solution to the aforementioned spectral congestion problem by introducing the opportunistic usage of the frequency bands that are not heavily occupied by licensed users [4], [5]. One of the most important features in the cognitive radio [6] is the ability to measure, sense, learn, and be aware of the parameters related to the radio channel characteristics. The primary users can be defined as the users who have a higher priority or legacy rights on the usage of a specific part of the available spectrum. On the other hand, the secondary users, who have a lower priority, exploit the spectrum in such a way that they do not cause interference to the primary users. Therefore, secondary users need to have *cognitive capabilities*, such as sensing the spectrum reliably to check if it is being used by a primary user so as to change the radio parameters for exploiting the unused part of the spectrum.

As a consequence, a working group named IEEE 802.22 was established to develop a standard for a cognitive radio based PHY/MAC/air interface to target on the license-exempt devices. The goal for these devices is to share the spectrum which has already been allocated to the digital television (DTV) broadcast services. The proposed system is called the *wireless regional area network* (WRAN), whose coverage area can be extended to as far as 30 miles. To implement the cognitive radio causing no interference with the licensed signals, users have to be able to detect the presence of the licensed signals even with very low signal-to-noise ratios (SNRs). The IEEE 802.22 WRAN group established a sensing tiger team to be responsible for spectrum sensing, including the spectrum sensing for the DTV signals modulated subject to the ATSC digital television standard [7], [8]. In addition, wireless microphones are the usual low-power secondary licensed signals operating in the locally unused DTV bands. Therefore, the main task in spectrum sensing for the IEEE 802.22 WRAN systems is to detect the existence of the DTV signals as well as the wireless microphone signals operating in the DTV frequency bands.

The target SNR for a good spectrum sensing sensitivity is about -20 dB [4], [9]–[13], which means that some of the licensed signals must be sensed at a very low SNR. This reflects the major challenge, *weak signal detection*, in spectrum sensing. In addition, fading and time dispersions of the wireless channel and noise/interference variations will also bring difficulties to spectrum sensing, such as signal energy fluctuation, noise uncertainty, and so on [1], [4], [14]–[16].

To combat the spectrum sensing problem with the above-mentioned difficulties, several methods have been proposed, such as the *matched filtering approach* [1], [14], [15], the *feature detection approach* [17], [18], and the *energy detection approach* [14], [19]–[22]. For the matched filtering technique, it can maximize the SNR. However, it is difficult to carry out the signal detection without information such as pilot and frame structure. For the feature detection method which relies on cyclostationarity, the sufficient signal information must be given as well. However, in practice, a cognitive radio receiver can not know anything about the primary signal's structure and information. On the other hand, for the energy detection method, although it does not require any information about the signal to be detected, it would be prone to the false detection since it only relies on the signal energy features [21], [22]. When the time-varying characteristics of the signal is obvious or noise is large [14], [15], [21], this method is likely to fail

Manuscript received 17 May 2010; revised 11 August 2010. This work was supported by Information Technology Research Award for National Priorities (NSF-ECCS 0426644), Networking Technology and Systems Award (NSF-CNS 0963793) from National Science Foundation, and DoD-DEPSCoR Grant (N0014-08-1-0856) from Office of Naval Research.

L. Lu and H.-C. Wu are with the Department of Electrical and Computer Engineering, Louisiana State University, Baton Rouge, LA 70803, USA (e-mail: {llu4@tigers.lsu.edu, wu@ece.lsu.edu}).

S. S. Iyengar is with the Department of Computer Science, Louisiana State University, Baton Rouge, LA 70803, USA (e-mail: iyengar@csc.lsu.edu).

Digital Object Identifier 10.1109/JSAC.2011.1102xx.

to distinguish between the absence and the presence of the signal. In addition, the energy detection scheme is not optimal for detecting the correlated (colored) signals, which are often found in practice. To overcome the shortcomings of the energy detection approach, some methods based on the eigenvalues associated with the covariance matrix of the received signal were proposed in [4], [9], [23]. However, the corresponding computational complexities are quite large. A method based on the higher-order-statistics (HOS) was proposed and it would be promising especially in the low SNR conditions [24]. In this paper, we propose a novel spectrum sensing scheme which is based on the Jarque-Bera (JB) statistic. The computational complexity of our new method is much less than the HOS approach while our method greatly outperforms the HOS technique over all SNR conditions and different signal sample sizes. Our method can perform very well even when the SNR is very low and the signal sample size is not large based on the Monte Carlo simulations. Our proposed new spectrum sensing technique would have a great potential to serve as the backbone of the future cognitive radio technology.

II. System Model

Denote the continuous-time received signal by $r_c(t)$ during the sensing stage. The underlying signal from the primary users is denoted by $s_c(t)$ and $w_c(t)$ is the additive white Gaussian noise (AWGN). Hence, we have

$$r_c(t) \stackrel{\text{def}}{=} s_c(t) + w_c(t). \tag{1}$$

Assume that we are interested in the frequency band with the central frequency f_c and the bandwidth W. We sample the received signal at a sampling rate f_s, where $f_s \geq W$. Let $T_s = \frac{1}{f_s}$ be the sampling period and N be the sample size. For notational convenience, we denote

$$\begin{aligned} r(n) &\stackrel{\text{def}}{=} r_c(nT_s), \ \ n = 1, \ldots, N, \\ s(n) &\stackrel{\text{def}}{=} s_c(nT_s), \ \ n = 1, \ldots, N, \\ w(n) &\stackrel{\text{def}}{=} w_c(nT_s), \ \ n = 1, \ldots, N. \end{aligned} \tag{2}$$

According to [4], for the signal detection (spectrum sensing) problem, there involve two hypotheses, namely H_0: signal is absent and H_1: signal is present. The discrete-time received signals under these two hypotheses are given by

$$H_0 : r(n) = w(n), \tag{3}$$

$$H_1 : r(n) = s(n) + w(n), \tag{4}$$

where $r(n)$ denotes the received signal samples including the effect of path loss, multipath fading and time dispersion, and $w(n)$ is the discrete-time AWGN with zero mean and variance σ^2. Here $s(n)$ can be the superposition of the signals emitted from multiple primary users. When the received signal $r(n)$ consists of multiple sources (from either multiple independent sources or a single source signal traveling through multiple paths), it is usually modeled as the *correlated signal* [4]. It is assumed that signal and noise are uncorrelated with each other. The spectrum sensing (or signal detection) problem is therefore to determine whether the signal $s(n)$ exists or not, based on the received signal samples $r(n)$ [4], [9]. In reality, the recorded DTV channels are sampled at $f_s = 21.524476$ MHz and then down-converted to a low central intermediate frequency (IF) of 5.381119 MHz (one fourth of the sampling frequency) [25]. The acquired signal samples are used to detect if any DTV signal exists.

III. Efficient Spectrum Sensing Techniques

The signal detection has been a fundamental but ever-intriguing problem in telecommunications, signal processing, etc. The Bayesian hypothesis test has served as the mainstream theoretical framework for signal detection. However, the Bayesian classifier can be deemed optimal only when the complete statistic information is known for the observed signal. It is impossible in practice. Besides, the accurate probability density function (or the complete statistic information), which facilitates the Bayesian optimality, has to depend on a large amount of data and it is not feasible for low-cost, low-power, computationally-efficient hand-held (mobile) devices. Instead of estimating the probability density function (PDF), the computationally-efficient detection methods using the partial statistics have been attracting a lot of research interest for decades. In this section, we first present an existing spectrum sensing technique based on the higher-order statistics. Then, we propose a novel spectrum sensing algorithm based on the JB-statistic, which is more robust than the former method especially when the sample size of the received signal is quite small.

A. Higher-Order-Statistics Spectrum-Sensing Algorithm

In this subsection, we will discuss about the higher-order-statistics (HOS) based detection algorithm (see [24]). This sensing technique is based on Gaussian noise statistics. The higher-order statistics can be used to evaluate how well the distribution of the test statistic matches a Gaussian distribution. In this method, the received signal is converted down to the baseband and then filtered. Next, the nominal ATSC pilot frequency is aligned to the DC and the down-converted signal is filtered again by a narrow-band low-pass filter. The resultant signal is transformed to the frequency domain using the fast Fourier transform (FFT). Often, a 2,048-point FFT is recommended, since it is also used in the OFDM modulator/demodulator for the digital video broadcasting systems. Then, the higher-order moments and cumulants (higher than the second-order) for the real and imaginary parts of the signal spectra are calculated. If only noise is present, then the real and imaginary parts of the signal spectra are both Gaussian. The corresponding higher-order cumulants are thus all zero. Hence, in this sensing technique, a *Gaussianity test* is performed using the estimates of the higher-order cumulants. If it fails the Gaussianity test, then the hypothesis that the ATSC pilot signal is present holds true. The HOS detection algorithm has to use the third- to sixth-order cumulants and central moments [24]. The estimation variances of such high-order cumulants are usually quite large especially when the sample size is small [26]. Hence, it is obvious that the HOS approach cannot be robust when we do not have much received signal data or the channel model is time-varying. It motivates us to design a new spectrum sensing method to combat this problem.

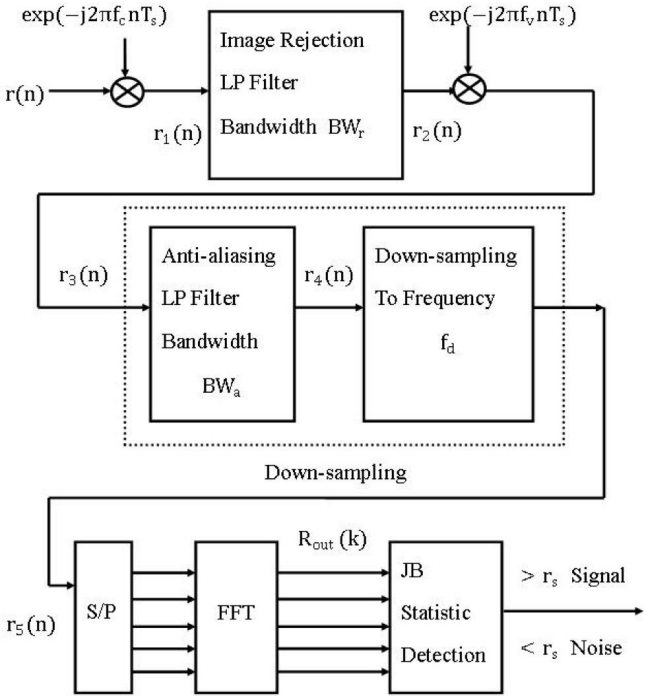

Fig. 1. The spectrum sensing system diagram.

B. Jarqur-Bera (JB) Statistic Based Detection Algorithm

Our goal is to design a robust spectrum sensing method involving estimates with less variances and leading to a computationally efficient solution. The JB statistic based on skewness and kurtosis is adopted here because kurtosis and skewness, which are composed by the second, third and fourth central moments only, could lead to more robust estimators than the HOS scheme relying on the higher-order moments or cumulants. Since JB statistic only depends on the second to fourth central moments, it would result in much less estimation variance than the variance of the HOS-based estimator (see [24], [26]) using the second to sixth cumulants and central moments altogether according to the k-statistic and h-statistic theory. In addition, the HOS detection method (see [24]) tests the normality using the real and imaginary parts of the complex received samples subject to the property that all higher-order cumulants of a Gaussian PDF are zero. We propose to adopt the JB statistic to work on the norms of the complex signal samples, and the associated normality test is thus subject to the Rayleigh distribution instead. It is well known that the variance of a Gaussian process (for either its real or imaginary part) is much larger than the variance of the corresponding Rayleigh process (constituting the absolute values of the complex Gaussian random data). Hence, it can be foreseen that our proposed spectrum sensing method based on the signal norms can have the advantage over the method in [24]. Our proposed new spectrum sensing algorithm will be presented subsequently in Sections III-B1- III-B3.

1) Pre-Processing: The pre-processing steps in our proposed algorithm for transforming the received signal $r(n)$ into the frequency domain are the same as the HOS detection method [24]. Nevertheless, in our new detection method, we use the Jarque-Bera statistic of the signal spectrum's absolute values. The block diagram of our proposed new spectrum sensing method is depicted in Figure 1.

The signal flow in Figure 1 is described as follows. When the signal $r(n)$ is received, first we multiply $r(n)$ by $e^{-j2\pi f_c n T_s}$ to down-convert it to the baseband, where f_c is the low central IF frequency of 5.381119 MHz. Then, this baseband signal is sent through a digital image rejection low-pass (LP) filter with bandwidth $BW_r = 8 \times 10^6 \times \frac{2\pi}{f_s}$ radians. The image rejection filter is placed in the receiver so that the image frequencies along with other unwanted signals are filtered out to enhance the signal quality.

Next, the enhanced signal $r_2(n)$ is further multiplied by $e^{-j2\pi f_v n T_s}$, where f_v=2.69 MHz. Then, the resulted signal $r_3(n)$ goes through the operations consisting of a down-sampler following a digital anti-aliasing filter whose bandwidth is given by

$$\mathrm{BW}_a = \frac{N_{\mathrm{FFT}}}{T_{\mathrm{sensing}}} \times \frac{2\pi}{f_s}, \tag{5}$$

where N_{FFT} is the FFT window size, and $T_{\mathrm{sensing}} = \frac{n}{f_s}$ is the sensing time. The down-sampling rate f_d is given by

$$f_d = \mathrm{floor}\left(\frac{2\pi}{BW_a}\right), \tag{6}$$

where the function "floor" is the operation to round $\frac{2\pi}{BW_a}$ to the nearest integer less than or equal to $\frac{2\pi}{BW_a}$. The down-sampled signal $r_5(n)$ is sent to a serial-to-parallel port and then the N_{FFT}-point FFT will be taken to result in a half-period FFT-sequence $R_{\mathrm{out}}(k)$, $k = 0, 1, \ldots, \frac{N_{\mathrm{FFT}}}{2} - 1$.

2) JB-Statistic Based Detection: In statistics, the Jarque-Bera test is a goodness-of-fit measure of departure from normality, based on the sample kurtosis and the sample skewness. The test is named after Carlos M. Jarque and Anil K. Bera. The test statistic, JB, is defined as

$$\mathrm{JB} \stackrel{\mathrm{def}}{=} \frac{n_s}{6}\left(\mathcal{S}^2 + \frac{(\mathcal{K}-3)^2}{4}\right), \tag{7}$$

where n_s is the number of observations (or degrees of freedom in general); $\mathcal{S}$ is the sample skewness and $\mathcal{K}$ is the sample kurtosis. They are defined as

$$\mathcal{S} \stackrel{\mathrm{def}}{=} \frac{\hat{\mu}_3}{\hat{\sigma}^3} = \frac{\hat{\mu}_3}{(\hat{\sigma}^2)^{3/2}} = \frac{\frac{1}{n_s}\sum_{i=1}^{n_s}(x_i - \bar{x})^3}{\left(\frac{1}{n_s}\sum_{i=1}^{n_s}(x_i - \bar{x})^2\right)^{3/2}}, \tag{8}$$

$$\mathcal{K} \stackrel{\mathrm{def}}{=} \frac{\hat{\mu}_4}{\hat{\sigma}^4} = \frac{\hat{\mu}_4}{(\hat{\sigma}^2)^2} = \frac{\frac{1}{n_s}\sum_{i=1}^{n_s}(x_i - \bar{x})^4}{\left(\frac{1}{n_s}\sum_{i=1}^{n_s}(x_i - \bar{x})^2\right)^2}, \tag{9}$$

where $\hat{\mu}_3$ and $\hat{\mu}_4$ are the estimates of the third and fourth central moments, respectively; x_i, $i = 1, \ldots, n_s$ are the observations; $\bar{x}$ is the sample mean and $\hat{\sigma}^2$ is the estimate of the second central moment or the variance. Therefore, this JB test can be considered as a sort of *portmanteau test*, since the four lowest moments about the origin are used jointly for its calculation.

Because $R_{\mathrm{out}}(k)$, $k = 0, 1, \ldots, \frac{N_{\mathrm{FFT}}}{2} - 1$ are complex-valued, if we try to directly apply JB test, we have to forsake either real-parts or imaginary-parts and thus the complete information is not utilized. For our proposed spectrum sensing method, we do not directly use the JB statistic as the

conventional approach thereby. Here we check the absolute values of $R_{\rm out}(k)$, $k = 0, 1, \ldots, \frac{N_{\rm FFT}}{2} - 1$. Then, we invoke Eqs. (7), (8), and (9) to calculate the JB statistic of $|R_{\rm out}(k)|$ and compare it with the threshold r_s to decide if there exists the signal $s(n)$. If JB $> r_s$, we say that the signal exists; otherwise (JB $\leq r_s$), we say that the signal is absent. We will present the theoretical study about how to select the threshold r_s subsequently.

3) Threshold Analysis for Our Proposed Method: In this subsection, we will discuss about how to select the threshold r_s for the proposed JB-statistic-based detection scheme according to both theoretical and heuristical analyses. Let's review the Rayleigh distribution first, which is closely related to our proposed feature $|R_{\rm out}(k)|$ under the JB test ($|R_{\rm out}(k)|$ is Rayleigh distributed when signal is absent). The Rayleigh distribution is composed by random complex numbers whose real and imaginary components (x and y) are both identically independently distributed (i.i.d.) Gaussian. The Rayleigh PDF with respect to $r = \sqrt{x^2 + y^2}$ is given by

$$f(r; \sigma_r) = \frac{r}{\sigma_r^2} \exp\left(\frac{-r^2}{2\sigma_r^2}\right), \tag{10}$$

where $r \in [0, +\infty)$, and σ_r is the mode. For the Rayleigh PDF given by Eq. (10), the skewness $\mathcal{S}_{\rm Rayleigh}$ and the kurtosis $\mathcal{K}_{\rm Rayleigh}$ are given as follows [27]:

$$\mathcal{S}_{\rm Rayleigh} = \frac{2\sqrt{\pi}(\pi - 3)}{(4 - \pi)^{\frac{3}{2}}} \approx 0.631, \tag{11}$$

$$\mathcal{K}_{\rm Rayleigh} = -\frac{6\pi^2 - 24\pi + 16}{(4 - \pi)^2} + 3 \approx -0.245 + 3 = 2.755. \tag{12}$$

When there is no signal, the input of the pre-processor (as presented in Section III-B1) is $r(n) = w(n)$. Then, after the pre-processing of the input signal, if there is no aliasing, the output $R_{\rm out}(k)$, $k = 0, 1, \ldots, \frac{N_{\rm FFT}}{2} - 1$ will be a complex Gaussian process whose real and imaginary components are both i.i.d. Gaussian. Thus, $|R_{\rm out}(k)|$, $k = 0, 1, \ldots, \frac{N_{\rm FFT}}{2} - 1$ will be Rayleigh-distributed. Substituting Eqs. (11) and (13) into Eq. (7), we can calculate the theoretical JB statistic value for Rayleigh distribution as $0.0344 N_{\rm FFT}$ (here we set $n_s = \frac{N_{\rm FFT}}{2}$). According to the central limit theorem and the law of large numbers, we know that when we apply different signal-absent observations ($r(n) = w(n)$) for λ times (λ is large enough), the JB statistic values in these different experiments will approximately satisfy a Gaussian distribution with a mean around $0.0344 N_{\rm FFT}$. That is, the distribution of these JB statistics will be approximately symmetric with respect to this mean. In addition, according to Eq. (7), the JB statistic is non-negative. It means that the smallest possible JB statistic value can only be zero, so subject to the symmetric property we can conclude that most (over 97% of the total population) of the JB statistic values will be smaller than twice of the mean $0.0344 N_{\rm FFT}$. On the other hand, if there is signal, $R_{\rm out}(k)$, $k = 0, 1, \ldots, \frac{N_{\rm FFT}}{2} - 1$ will not satisfy a Gaussian distribution. Thus, the skewness and the kurtosis of $|R_{\rm out}(k)|$, $k = 0, 1, \ldots, \frac{N_{\rm FFT}}{2} - 1$ would become larger. According to the aforementioned analysis, we set the threshold r_s for our JB-statistic based detector as

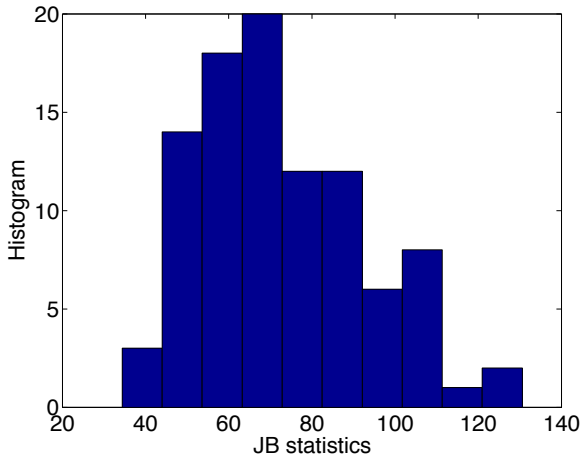

Fig. 2. A histogram example of the JB statistics.

$$r_s = 0.0688 N_{\rm FFT}. \tag{13}$$

For instance, when we select $N_{\rm FFT} = 2,048$, which is the defaulted FFT window size according to the DVB standards, the threshold will be $r_s = 141$. Figure 2 depicts the histogram of the JB statistics for a complex Gaussian process over 1,000 random experiments. It can be clearly seen that all JB statistic values in Figure 2 are below the threshold $r_s = 141$. In addition, the ensemble means of the calculated JB statistics and the (false-alarm) percentages of the JB statistics larger than $r_s = 141$ are listed in Table I. Provably, when the FFT window size is chosen as 2,048, the means of the JB statistics are always close to $0.0344 * 2048$. Its double, $r_s = 141$, can be selected as the threshold, and the corresponding false alarms are always very small. Note that this threshold selection does not depend on the sample size N.

IV. Normality and Spectral Analysis

Via the thorough numerical evaluation, it is discovered that the performances of both our proposed JB detection method and HOS detection scheme significantly vary with respect to the sample size. The larger the sample size, the better the detection results. The HOS detection scheme is much more sensitive to the sample size. When the sample size is not sufficiently large (below 70,000), the HOS detection method would lead to a very high false alarm rate and fail. On the other hand, our proposed JB detection method can still lead to satisfactory results for the sample size is around 30,000. The reason is that when the sample size is small, $R_{\rm out}(k)$, $k = 0, 1, \ldots, N_{\rm FFT} - 1$ may not constitute a Gaussian process even in the sole presence of AWGN. To explain this interesting phenomenon, we first employ the Gaussianity test for the received signal involving the AWGN only.

The received signal spectral waveform as illustrated in

TABLE I
JB STATISTIC ANALYSIS

	Sample Size N					
	150,000	200,000	250, 000	300,000	350,000	400,000
Mean	73.5	75.6	72.5	76.3	74.2	74.3
False-Alarm Percentage (JB >141)	1%	2%	4%	3%	2%	3%

Figure 1 is given by

$$\begin{aligned} R_{\rm out}(k) &= \mathbf{Re}\left\{R_{\rm out}(k)\right\} + \sqrt{-1}\ \ \mathbf{Im}\left\{R_{\rm out}(k)\right\} \\ &= \sum_{n=0}^{N_{\rm FFT}-1} \cos\left(\frac{2\pi kn}{N_{\rm FFT}}\right) r(n) \qquad (14) \\ &\quad + \sqrt{-1}\sum_{n=0}^{N_{\rm FFT}-1} \sin\left(\frac{2\pi kn}{N_{\rm FFT}}\right) r(n), \\ &\quad k = 0, 1, \ldots, \frac{N_{\rm FFT}}{2} - 1. \qquad (15) \end{aligned}$$

Note that for the HOS detection method, we have to use the full-period $R_{\rm out}(k)$, $k = 0, 1, \ldots, N_{\rm FFT} - 1$ instead. According to Eq. (14), we can measure the normalities separately for the real and imaginary parts of $R_{\rm out}(k)$. The following subsections are presented to study why $R_{\rm out}(k)$, $k = 0, 1, \ldots, N_{\rm FFT} - 1$ do not satisfy the Gaussian assumption.

A. Edgeworth Expansion for PDF Characterization

As previously stated, the small sample size would often lead to the non-Gaussian characteristics of the received signals even in the sole presence of AWGN [28]. The Edgeworth expansion has been used to characterize the unknown PDF based on the estimated moments and cumulants. We adopt the Edgeworth expansion (see [29], [30]) to model the actual PDF of the aforementioned signal $\mathbf{Re}\left\{R_{\rm out}(k)\right\}$ and then evaluate the mismatch between the actual PDF and the underlying Gaussian model. Similar techniques can be used to study the statistical behavior for $\mathbf{Im}\left\{R_{\rm out}(k)\right\}$ as well and we omit this redundant discussion.

For a random variable Z ($Z = \mathbf{Re}\left\{R_{\rm out}(k)\right\}$ in our application here) with $E\{Z\}= 0$ (this can always be achieved by creating a mean-removed variable $Z - E\{Z\}$) and unit variance, the arbitrary probability density function for Z can be written by Edgeworth expansion as [29], [30]:

$$f_Z(z) = \vartheta(z)\left\{1 + \sum_{k=1}^{+\infty} P_k(z)\right\}, \qquad (16)$$

where $\vartheta(z)$ is the zero-mean univariate Gaussian PDF, which is given by

$$\vartheta(z) \stackrel{\rm def}{=} \frac{1}{\sqrt{2\pi}} \exp\left(-\frac{z^2}{2}\right), \qquad (17)$$

and $P_k(z)$ is a polynomial such that

$$P_k(z) \stackrel{\rm def}{=} \sum_{\{l_m\}} H_{k+2\varpi}(z) \prod_{m=1}^{k} \frac{1}{l_m!}\left(\frac{\chi_{m+2}}{(m+2)!}\right)^{l_m}. \qquad (18)$$

Here the set $\{l_m\}$ consists of all non-negative integer solutions to the equation $l_1+2l_2+\ldots+kl_k = k$, and $\varpi = l_1+l_2+\ldots+l_k$. Note that χ_l is the $l^{\rm th}$-order cumulant of $\mathbf{Re}\left\{R_{\rm out}(k)\right\}$, which is given by

$$\chi_l = (-1)^l \frac{d^l}{d\eta^l} \log \hat{f}_Z(\eta)\Big|_{\eta=0}, \qquad (19)$$

where $\hat{f}_Z(\eta) \stackrel{\rm def}{=} E\left\{e^{jz\eta}\right\}$ is the characteristic function of $\mathbf{Re}\left\{R_{\rm out}(k)\right\}$ and $H_l(z)$ is the $l^{\rm th}$-order Hermite polynomial such that

$$\vartheta(z)H_l(z) = (-1)^l \frac{d^l}{dz^l}\vartheta(z). \qquad (20)$$

Later on, we will compare the actual PDF given by Eq. (16) with the Gaussian model given by Eq. (17) for $Z = \mathbf{Re}\left\{R_{\rm out}(k)\right\}$ to test if there is significant statistical mismatch in between.

B. Gaussianity Measure Using KGGS Test

Although the Edgeworth expansion can help us to obtain the complete "actual PDF", it cannot provide a simple (scalar) measure for the aforementioned mismatch in practice. Recently, we proposed a robust Gaussianity measure, namely *Kullback-Leibler-Divergence Gaussian Generalized-Gaussian Skewness* (KGGS) test [31]. Note that in the following analysis, for the JB detection method, the sample size is $M = \frac{N_{\rm FFT}}{2}$ while for the HOS detection method, the sample size is $M = N_{\rm FFT}$ instead. The two underlying PDF models used in our KGGS test are specified as follows.

1) Gaussian PDF:

$$q(z) = q_G(z) \stackrel{\rm def}{=} \frac{1}{\sigma\sqrt{2\pi}} \exp\left(-\frac{(z-\mu)^2}{2\sigma^2}\right), \qquad (21)$$

where μ is the mean and σ^2 is the variance of the sequence $z(1), ..., z(M)$;

2) Generalized Gaussian (GG) PDF:

$$q(z) = q_{\rm GG}(z;\alpha,\beta) \stackrel{\rm def}{=} \frac{\beta}{2\alpha\,\Gamma\left(\frac{1}{\beta}\right)} \exp\left\{-\frac{|z|^\beta}{\alpha}\right\}, \qquad (22)$$

where α characterizes the width of the PDF peak (or standard deviation), β is inversely proportional to the functional decreasing rate from the peak value, and $\Gamma(\ )$ denotes the Gamma function. Very often, α is referred to as the *scale parameter*, while β is called the *shape parameter*.

Next, let's simply introduce the KGGS test here. Suppose that the observations $z(i), i = 1, \ldots, M$ are drawn from a stationary random process Z whose true PDF $f(z)$ is unknown. We wish to find if these data fit the normal (Gaussian) distribution. According to [31], we can use the sample average of $\log\left(q(z(i))\right)$ to determine how well the model PDF $q(z)$ fits the underlying random process. In addition, according to [31], the Gaussian PDF model is a special case of the generalized Gaussian model with $\beta = 2$. It means that if

we use both Gaussian and generalized Gaussian PDF models ($q_1(z)$ and $q_2(z)$ respectively) to fit the observations with the true normal distribution, then theoretically speaking, we get $f(z) = q_1(z) = q_2(z)$ and thus $\int_{-\infty}^{\infty} f(z)\log(q_1(z))\,dz = \int_{-\infty}^{\infty} f(z)\log(q_2(z))\,dz$. As the sample size approaches to infinity ($M \to \infty$), there will appear to be very little difference between the sample averages of $\log(q_1(z(i)))$ and $\log(q_2(z(i)))$. However, for a random process Z whose actual PDF $f(z)$ is not Gaussian, such difference would not be negligible. Hence we can establish a new rule based on this difference in the two sample means of the two populations $\log(q_1(z(i)))$ and $\log(q_2(z(i)))$ to determine if the true PDF $f(z)$ of the random process Z is the normal distribution. The steps for our proposed new Gaussianity test are stated as follows:

Step 1) Use the Gaussian PDF to fit the observations $z(i), i = 1,\ldots,M$; estimate the sample mean $\hat{\mu}$ and the sample variance $\hat{\sigma^2}$, and obtain the values of $\log(q_1(z(i)))$, for $i = 1,2,\ldots,M$, where $q_1(z) = 1/(\hat{\sigma}\sqrt{2\pi})\exp\big(-(z-\hat{\mu})^2/(2\hat{\sigma^2})\big)$.

Step 2) Use the generalized Gaussian PDF to fit the observations instead and calculate the values of $\log(q_2(z(i)))$, for $i = 1,2,\ldots,M$, where $q_2(z) = q_{\rm GG}(z;\hat{\alpha},\hat{\beta})$ is defined by Eq. (22). Note that the parameters $\hat{\alpha}$, $\hat{\beta}$ are estimated according to [31].

Step 3) Establish the statistic Υ as follows and use the composite rule in [31] to determine whether $f(z)$ is Gaussian or not:

$$\Upsilon = \left|\left[\frac{1}{M}\sum_{i=1}^{M}\log(q_1(z(i))) - \frac{1}{M}\sum_{i=1}^{M}\log(q_2(z(i)))\right]^{0.05}\right|. \quad (23)$$

We propose to use the KGGS test stated above for the robustness analysis of both our JB detection method and the HOS detection scheme. The application of this new analysis for spectrum sensing can be manifested in Section VI.

C. Spectral Analysis

As previously mentioned, our JB detection method depends on $|R_{\rm out}(k)|$, $k = 0,1,\ldots,\frac{N_{\rm FFT}}{2}-1$, but the HOS detection method depends on $R_{\rm out}(k)$, $k = 0,1,\ldots,N_{\rm FFT}-1$ instead. In this subsection, we will explain the reason why our method does not rely on $R_{\rm out}(k)$, $k = 0,1,\ldots,N_{\rm FFT}-1$ as the HOS detection method. The frequency spectrum of the sampled received DTV signal $r(n)$ has a bandwidth of $6\times10^6\times\frac{2\pi}{f_s}$ radians and a central frequency $5.38119\times10^6\times\frac{2\pi}{f_s}$ radians according to [25] (see details in Section VI). According to Figure 1, after down-conversion, image rejection and frequency shifting, the spectrum of the signal $r_3(n)$ will occupy the digital frequency intervals ranging from 0 to $5.69\times10^6\times\frac{2\pi}{f_s} = 0.5288\pi$ radians (with a bandwidth 0.5288π radians) over $[0,\pi]$, and ranging from $2\pi-(6-5.69)\times10^6\times\frac{2\pi}{f_s} = 1.9712\pi$ to 2π radians (with a bandwidth 0.0288π) over $[\pi,2\pi)$. Due to the frequency-shifting operations in Figure 1, it can be seen that the magnitude spectrum of $r_3(n)$ is definitely not symmetric over $[-\pi,\pi]$. Next, let the signal $r_3(n)$ pass the low-pass filter with a bandwidth BW_a specified by Eq. (5), and down-sample $r_4(n)$ with a down-sampling rate f_d given by Eq. (6). The half-period FFT sequence $R_{\rm out}(k)$, $k = 0,1,\ldots,\frac{N_{\rm FFT}}{2}-1$ should correspond to the digital frequency interval $[0,\pi]$ in where $|R_{\rm out}(k)|$ would not have any null band. However, the signal spectrum $R_{\rm out}(k)$, $k = \frac{N_{\rm FFT}}{2},\frac{N_{\rm FFT}}{2}+1,\ldots,N_{\rm FFT}-1$ corresponding to $[\pi,2\pi)$ would exhibit a null band especially when the sample size N is smaller than the threshold number ν (ν will be defined in Eq. (24)) which makes the low-pass filter possess a bandwidth of 0.0288π radians (this bandwidth is identical to the signal bandwidth within $[\pi,2\pi)$). In other words, we will have $R_{\rm out}(k) = 0$, for some k values when the sample size N is smaller than ν. Besides, if the null band of $R_{\rm out}(k)$ is too broad, $R_{\rm out}(k)$, $k = 0,1,\ldots,N_{\rm FFT}-1$ would not fit the complex Gaussian distribution even in the sole presence of AWGN. Thus when the sample size N is not large enough, if we use the full-period $R_{\rm out}(k)$, $k = 0,1,\ldots,N_{\rm FFT}-1$ for the spectrum sensing, it will lead to a very high false alarm rate and the result is not satisfactory. This is the very reason why the HOS detection method often leads to a very high false alarm rate when the sample size N is small. It is also the reason why our JB detection scheme should rely on the half-period $R_{\rm out}(k)$, $k = 0,1,\ldots,\frac{N_{\rm FFT}}{2}-1$. Based on the previous discussion, the theoretical value for ν can be calculated as

$$\nu = \frac{\pi}{0.0288\pi}\times N_{\rm FFT}. \quad (24)$$

Eq. (24) facilitates the sample size N for the down-sampling rate $f_d = \frac{\pi}{0.0288\pi}$. In other words, the minimum sample size $N = \nu$ is required for the HOS detection method to work. For example, when the FFT window size is set as $N_{\rm FFT} = 2048$, we need $N \geq \nu \approx 71,000$. The effects of sample size can also be found in our previous discussions in Sections IV-A, IV-B and in the subsequent Section VI.

V. Computational Complexity Analysis

The computational complexity is always an important factor to be considered in practice. Therefore, the computational complexity studies for our JB detection method and HOS detection method are presented in this section. For simplicity, here we only consider the real-valued multiplications in studying the complexity. Thus, the computational complexity analysis for the two aforementioned detectors is presented as follows. For our proposed JB statistic-based detector, we need to take $4\times\frac{N_{\rm FFT}}{2}$ multiplications to calculate the absolute values of $R_{\rm out}(k)$, $0,1,\ldots,\frac{N_{\rm FFT}}{2}-1$. Moreover, in order to obtain $\mathcal{S}$ and $\mathcal{K}$ in Eqs. (8) and (9), we need to compute the second, third, and fourth moments of $|R_{\rm out}(k)|$, $0,1,\ldots,\frac{N_{\rm FFT}}{2}-1$. Hence, we need to take $3\times\frac{N_{\rm FFT}}{2}$ multiplications for achieving that. At last, we need one more comparison operation to carry out the ultimate hypothesis test. In total, for our JB statistic-based detection, the complexity $\mathbb{C}_{\rm JB}$ (in terms of multiplications) is given by

$$\mathbb{C}_{\rm JB} = 7\times\frac{N_{\rm FFT}}{2}+1 = 3.5\,N_{\rm FFT}+1. \quad (25)$$

The HOS detection method in [24] depends on $R_{\rm out}(k)$, $k = 0,1,\ldots,N_{\rm FFT}-1$. It needs to take $10\times N_{\rm FFT}$ multiplications to calculate the second to sixth moments of both

real and imaginary parts of $R_{\rm out}(k)$. Furthermore, it needs 10 multiplications to calculate the required cumulants, and needs to take 3 comparison operations for the ultimate hypothesis test. Therefore, its total computational complexity $\mathbb{C}_{\rm HOS}$ is

$$\mathbb{C}_{\rm HOS} = 10 \times N_{\rm FFT} + 13. \tag{26}$$

Usually, we choose $N_{\rm FFT}$ to be 2,048, so it is obvious that our proposed JB-statistic based detector is much more computationally efficient than the HOS detector. We also depict the trends of the computational complexities versus different $N_{\rm FFT}$ for these two detectors in the next section.

VI. Simulation

In our simulation, we test two types of commonly-used signals, namely DTV signal and microphone signal to benchmark the spectrum sensing methods. The simulation details are stated as follows.

A. Signal Acquisition and System Set-up

Subject to the IEEE 802.22 standard, the recorded DTV channels were sampled at 21.524476 Msamples/sec and then down-converted to a low central IF frequency of 5.381119 MHz (a fourth of the sampling rate). The real DTV data were acquired from [9]. On the other hand, according to [32], we simulate the microphone signal $s_{\rm mic}(t)$ as follows:

$$s_{\rm mic}(t) = \cos\left(2\pi \int_0^t \left[f_{cm} + f_{\triangle}\, w_m(\tau)\right] d\tau\right), \tag{27}$$

where f_{cm} is the same frequency as that of the DTV pilots; $f_{\triangle}$ is the frequency deviation around 100 KHz; $w_m(\tau)$ is the source signal which is randomly generated from the uniformly-distributed number in (-1,1). In addition, the sampling frequency for $s_{\rm mic}(t)$ is 21.524476 MHz, which is the same as that of the captured DTV signal.

According to [33], [34], the receiver noise characteristic consists of a typical noise power spectral density (PSD) and a noise uncertainty. The noise uncertainty specification is necessary since even though the sensing mechanism may involve calibration based on the noise power estimation, the estimate often exhibits some inaccuracy, which must be modeled. The thermal noise PSD is $N_0 = -174$ dBm/Hz. The receiver noise level is larger than the thermal noise level. Considering the effects of low-noise amplifier (LNA) noise figure, coupling losses, radio frequency (RF) switch losses and other issues, the TV industry typically specifies a *composite receiver noise figure* of 11 dB. Hence the average receiver noise PSD is $\bar{N} = N_0 + 11 = -163$ dBm/Hz.

Moreover, according to the IEEE 802.22 document [25], for the purpose of employing the captured signal to evaluate different detection schemes, it is necessary to initially process the captured ATSC-DTV signals. In particular, the SNR can be precisely controlled in the same way by using this initial process for all different spectrum sensing methods. Quoted from [25], the specific steps for the initial process are given as follows.

Step 1): Read an appropriate number of samples from one of the DTV signal files.

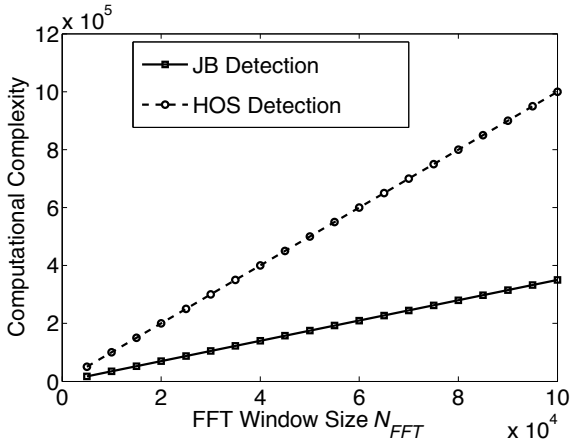

Fig. 3. Computational complexity measures versus N_{FFT} for our proposed JB detector and the HOS detector.

Step 2): Filter the signal using a passband filter with a 6 MHz bandwidth and a center frequency of 5.38119 MHz. The filter shall be a "brick wall" filter (i.e. it shall have a flat frequency response with unity gain) which can allow some rare exceptions.

Step 3): Measure the power in the received signal.

Step 4): Generate white noise sampled at 21.524476 MHz and filter it through the same filter used in Step 2. The noise power used is the receiver noise power.

Step 5): Scale the signal power to meet the target SNR.

Step 6): Add the filtered noise with the scaled and filtered signal.

B. Spectrum Sensing Performance Comparison

In the following, we will present the simulation results for comparing our JB-statistic based detector and the HOS detector. First, the wireless microphone signals according to [9], [32] (randomly generated from computer) and the captured DTV signals from [9] (from the real world) are generated for the benchmark. In the simulation, we set $N_{\rm FFT} = 2048$, which is also used in the OFDM modulator/demodulator, except that in Figure 3, $N_{\rm FFT}$ may vary. To the best of our knowledge, the required sample size N is at least 100,000 for almost all existing spectrum sensing techniques [1], [4], [5], [9], [24]. However, our proposed JB detection method can easily rely on the relatively much smaller sample size around $N = 30,000$ to achieve satisfactory results.

In Figure 2, we set the sample size N as 150,000 and depict the histogram of the JB statistic values from 1000 random experiments. The associated means and the false-alarm rates (for the JB statistics which are larger than $r_s = 141$) are listed in Table I for different N values. In Figure 4, we delineate the false detection rates resulting from the HOS detector and our JB-statistic based detector versus the sample size N in the sole presence of AWGN. According to Figure 4, it is obvious that when the sample size is larger than 50,000, both our JB-statistic based detector and the HOS detector have very low false detection rates. As the sample size gets smaller (< 50000), in other words, when the sensing time

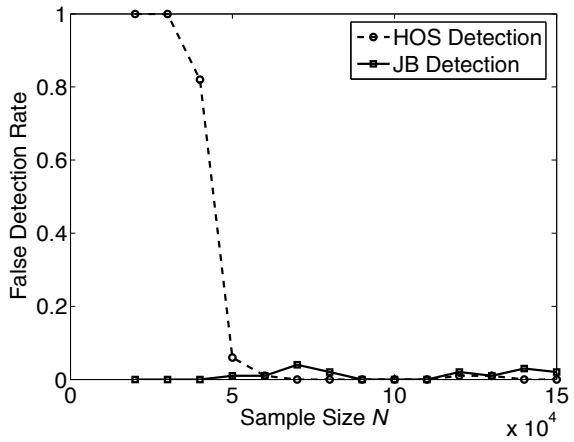

Fig. 4. False detection rate versus sample size in the sole presence of AWGN.

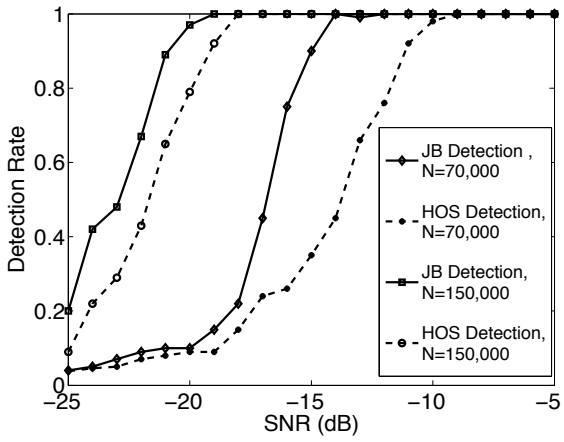

Fig. 6. Detection rate for real DTV signals versus SNR in the single-source case.

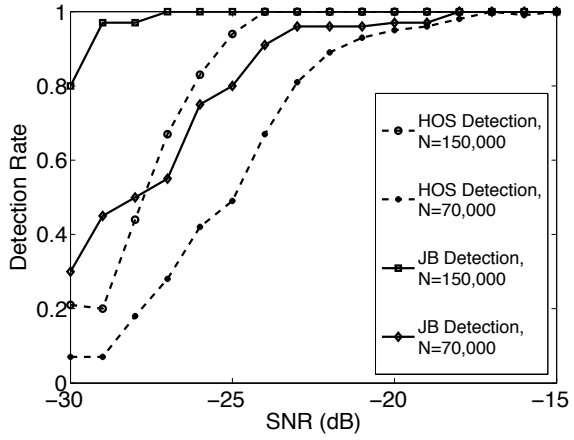

Fig. 5. Detection rate for simulated wireless microphone signals versus SNR in the single-source case.

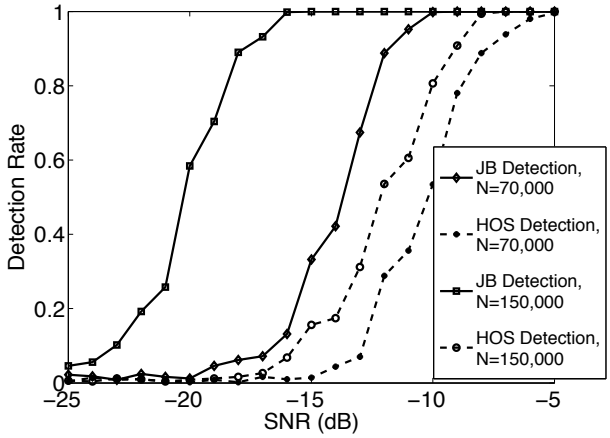

Fig. 7. Detection rate for real DTV signals versus SNR in the two-source case.

is short, the HOS detector leads to an extremely high false detection rate. Nevertheless, our proposed JB-statistic based detector can still work very well. In Figure 5, we depict the detection rates for the simulated wireless microphone signals from a single source over 1000 Monte Carlo experiments with $N = 70,000$ and $N = 150,000$, respectively. In Figure 6, we plot the detection rates for the real DTV signals from a single source over 1000 Monte Carlo experiments with $N = 70,000$ and $N = 150,000$, respectively. According to Figures 5 and 6, for the single-source case, our JB-statistic based detector always outperforms the HOS detector across different signal-to-noise ratios in terms of detection rate. Next, we will explore the multiple-source case, where the received signal is the correlated signal. In Figure 7, we plot the detection rates for the real DTV signals collected from two sources over 1000 Monte Carlo experiments with $N = 70,000$ and $N = 150,000$, respectively. In this case, our JB-statistic based detector leads to a much better performance than the HOS detector, even when the sample size for the former method is 70,000 but that for the latter technique is 150,000. Obviously, the HOS detector does not work very well for the correlated signals.

In Figures 8 and 9, we use the Edgeworth expansion and the Gaussian model to characterize the PDFs for the full-period signal sequence $Z = R_{\rm out}(k)$, $k = 0, 1, \ldots, N_{\rm FFT} - 1$ and the half-period signal sequence $Z = R_{\rm out}(k)$, $k = 0, 1, \ldots, \frac{N_{\rm FFT}}{2} - 1$ in the sole presence of AWGN ($r(n)$=$w(n)$). The sample sizes in Figure 8 and Figure 9 are $N = 30000$ and $N = 70000$, respectively. For these two sets of data, we perform the KGGS test to check the normality. The results of the KGGS test are given in Table II. According to Table II, the rejection percentages are very high for the normality assumption when the sample size N is not large enough. It clearly shows that the raw feature of $R_{\rm out}(k)$ used in the HOS detector is not robust when only a few dozens of thousands of samples are acquired or when the sensing time is short. To get more insights into this discovery, we provide Figures 10 and 11 to show the magnitude frequency spectra $|R_{\rm out}(k)|$, $k = 0, 1, \ldots, N_{\rm FFT} - 1$ for $N = 30000$ and $N = 70000$, respectively. It can be easily seen that there exist *null bands* in the signal spectra as depicted by Figures 10 and 11 and such null bands would easily destroy

TABLE II
REJECTION RATES OF KGGS NORMALITY TEST

	N						
	20,000	30,000	40, 000	50,000	60,000	70,000	80,000
$M = N_{\rm FFT}$	100%	100%	100%	100%	100%	11%	0%
$M = \frac{N_{\rm FFT}}{2}$	76%	12%	8%	7%	7%	5%	0%

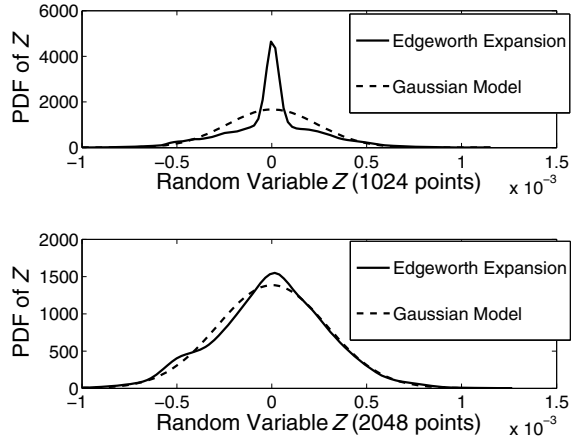

Fig. 8. The actual PDF resulting from the Edgeworth expansion and the PDF using the underlying Gaussian model for received data ($N = 30,000$, $N_{\rm FFT}$=2048).

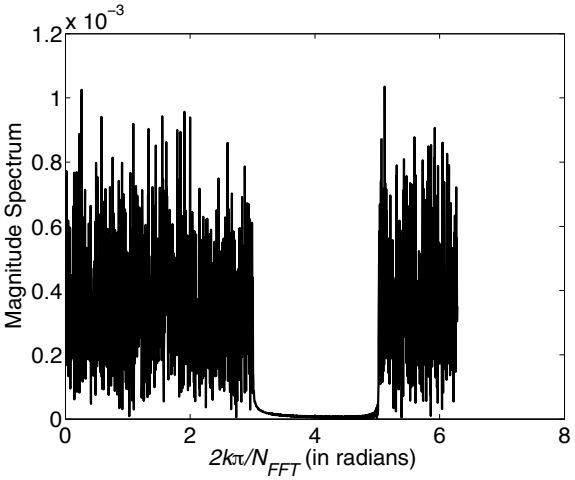

Fig. 10. $|R_{\rm out}(k)|$ versus frequency $\frac{2k\pi}{N_{\rm FFT}}$ ($N = 30,000$).

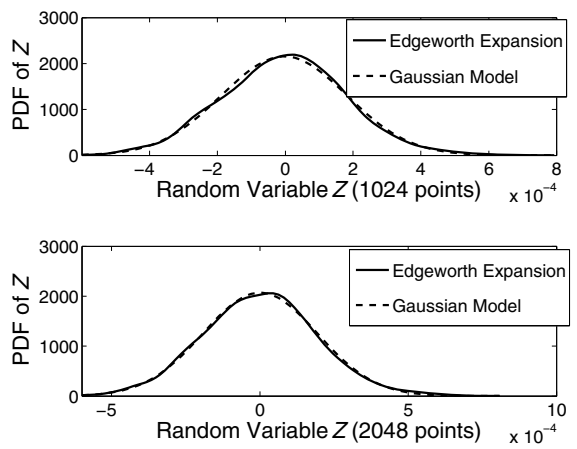

Fig. 9. The actual PDF resulting from the Edgeworth expansion and the PDF using the underlying Gaussian model for received data ($N = 70,000$, $N_{\rm FFT}$=2048).

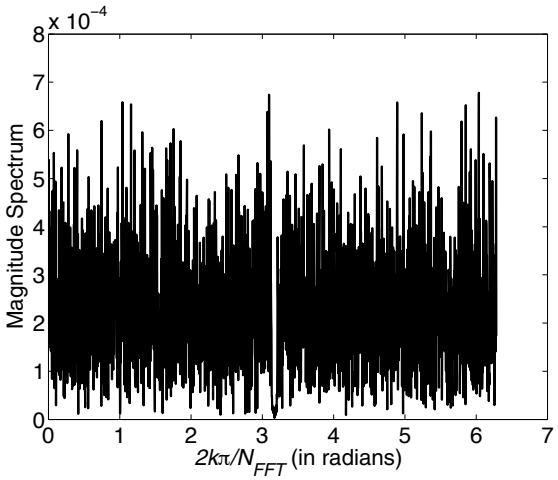

Fig. 11. $|R_{\rm out}(k)|$ versus frequency $\frac{2k\pi}{N_{\rm FFT}}$ ($N = 70,000$).

the normality and degrade the detection performance. Besides, the bandwidth of such a null band increases as the sample size decreases. Hence, the full-period feature $R_{\rm out}(k)$ adopted in the HOS detector may not lead to robust performance. According to Figures 8-11 and Table II, we can justify our arguments stated in Section IV. When the sample size N is not sufficiently large, the underlying full-period feature $R_{\rm out}(k)$, $k = 0, 1, \ldots, N_{\rm FFT} - 1$ used in the HOS detector does not satisfy the Gaussian assumption, but the half-period feature $R_{\rm out}(k)$, $k = 0, 1, \ldots, \frac{N_{\rm FFT}}{2} - 1$ would much better fit the Gaussian hypothesis. Next we would like to investigate how the HOS detector performs if it also uses the half-period feature $R_{\rm out}(k)$, $k = 0, 1, \ldots, \frac{N_{\rm FFT}}{2} - 1$. In Figure 12, we use the half-period feature $R_{\rm out}(k)$, $k = 0, 1, \ldots, \frac{N_{\rm FFT}}{2} - 1$ instead in the HOS detector and depict the corresponding detection rates. The similar performance results to those arising from the aforementioned HOS detector (when the full-period feature $R_{\rm out}(k)$, $k = 0, 1, \ldots, N_{\rm FFT} - 1$ is used) are shown. However, the detection rates are lower than the results from our proposed JB statistic based detector. To compare the complexity measures in numerical illustration, Figure 3 depicts the computational complexities in terms of multiplications for the HOS detection method and our proposed detector. It clearly shows that our method is much more efficient.

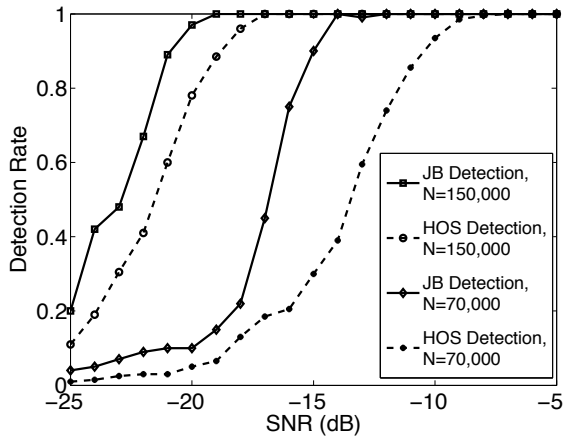

Fig. 12. Detection rate for real DTV signals versus SNR in the single-source case when the JB detector and the HOS detector are both based on the half-period feature $R_{\text{out}}(k)$, $k = 0, 1, \ldots, \frac{N_{\text{FFT}}}{2} - 1$.

VII. Conclusion

In this paper, we propose a novel JB-statistic based spectrum sensing method, which can be applied for the IEEE 802.22 systems. Our method outperforms the existing HOS detection scheme which is based on the higher-order statistics. According to our Monte Carlo simulation results for the simulated wireless microphone signals and the real DTV signals, our proposed JB detection method not only leads to a higher detection rate but also induces less computational complexity than the HOS detector. Besides, our proposed JB-statistic based detector can be very robust for the small sample size or the short sensing time. We also provide the normality analysis and the spectral analysis to explore the reasons why our proposed detector has the significant advantages over the HOS detection method especially when the sample size is small.

VIII. Acknowledgment

The authors greatly appreciate Drs. Ying-Chang Liang and Yonghong Zeng for their kind help on the data acquisition and the invaluable guidance to enable this work. The authors also dedicate this paper to Professor Sanjit K. Mitra for his inspirational and pioneering work on signal processing.

References

[1] D. Cabric, A. Tkachenko, and R. W. Brodersen, "Spectrum sensing measurements of pilot, energy, and collaborative detection," in *Proc. IEEE Military Communications Conference*, October 2006, pp. 1–7.

[2] Y.-C. Liang, H.-H. Chen, J. Mitola, P. Mahonen, R. Kohno, J. H. Reed, and L. Milstein, "Guest editorial - cognitive radio: Theory and application," *IEEE J. Sel. Areas Commun.*, vol. 26, no. 1, pp. 1–4, May 2008.

[3] L. Zhang, Y.-C. Liang, and Y. Xin, "Joint beamforming and power allocation for multiple access channels in cognitive radio networks," *IEEE J. Sel. Areas Commun.*, vol. 26, no. 1, pp. 38–51, January 2008.

[4] Y. H. Zeng and Y.-C. Liang, "Eigenvalue based spectrum sensing algorithms for cognitive radio," *IEEE Trans. Commun.*, vol. 57, no. 6, pp. 1784–1793, June 2009.

[5] T. Yucek and H. Arslan, "A survey of spectrum sensing algorithms for cognitive radio applications," *IEEE Commun. Surveys & Tutorials*, vol. 11, no. 1, pp. 116–130, March 2009.

[6] Y.-C. Liang and F. Chin, "Two suboptimal algorithms for downlink beamforming in FDD DS-CDMA mobile radio," *IEEE J. Sel. Areas Commun.*, vol. 19, no. 7, pp. 1264–1275, July 2001.

[7] H. S. Chen, W. Gao, and D. G. Daut, "Spectrum sensing for wireless microphone signals," in *Proc. 5th IEEE Annual Communications Society Conference on Sensor, Mesh and Ad Hoc Communications and Networks Workshops*, June 2008, pp. 1–5.

[8] *ATSC Digital Television Standard, Revision E with Amendments No. 1 and No. 2*, Std., 2005.

[9] Y.-C. Liang, Y. H. Zeng, E. C. Y. Peh, and A. T. Hoang, "Sensing-throughput tradeoff for cognitive radio networks," *IEEE Trans. Wireless Commun.*, vol. 7, no. 4, pp. 1326–1337, April 2008.

[10] M. Ghosh, V. Gaddam, and G. Turkenich, *DTV Signal Sensing Using Pilot Detection*, IEEE Std. 802.22-07/0125-00-0000, March 2007.

[11] C. W. Einolf, *Protection Criteria in the Broadcast Bands*, IEEE Std. 802.22-07/0223r0, May 2007.

[12] K. PO and J. TAKADA, "Conservative protection criteria for TV broadcasting services from ieee 802.22 WRAN," in *3rd International Conference on Cognitive Radio Oriented Wireless Networks and Communications*, May 2008, pp. 1–4.

[13] G. Chouinard, *Use of collaborative sensing to reduce false positive results*, IEEE Std. 802.22-08/0118r0, May 2008.

[14] A. Sahai and D. Cabric, "Spectrum sensing: fundamental limits and practical challenges," in *IEEE International Symposium on New Frontiers Dynamic Spectrum Access Networks*, November 2005.

[15] H. S. Chen, W. Gao, and D. G. Daut, "Signature based spectrum sensing algorithms for IEEE 802.22 WRAN," in *Proc. IEEE International Conference on Communications (ICC)*, June 2007, pp. 6487–6492.

[16] A. Sahai, N. Hoven, and R. Tandra, "Some fundamental limits on cognitive radio," in *Proceedings of 42nd Allerton Conference on Communication, Control, Computing*, October 2004, pp. 131–136.

[17] S. Enserink and D. Cochran, "A cyclostationary feature detector," in *Proceedings of Asilomar Conference on Signals, Systems and Computers*, vol. 2, October-November 1994, pp. 806–810.

[18] Y. P. Lin and C. He, "Subsection-average cyclostationary feature detection in cognitive radio," in *Proc. International Conference on Neural Networks and Signal Processing*, July 2008, pp. 604–608.

[19] S. M. Kay, *Fundamentals of Statistical Signal Processing: Detection Theory*. Upper Saddle River, New Jersey: Prentice-Hall, 1998.

[20] S. J. Shellhammer, S. Shankar, R. Tandra, and J. Tomcik, "Performance of power detector sensors of DTV signals in IEEE 802.22 WRANs," in *Proceedings of the Fist International Workshop on Technology and Policy for Accessing Spectrum (TAPAS)*, August 2006.

[21] A. Sonnenschein and P. M. Fishman, "Radiometric detection of spread-spectrum signals in noise of uncertainty power," *IEEE Trans. Aerospace Electron. Syst.*, vol. 28, no. 3, pp. 654–660, July 1992.

[22] R. Tandra and A. Sahai, "Fundamental limits on detection in low SNR under noise uncertainty," in *Proc. International Conference on Wireless Networks, Communications and Mobile Computing*, vol. 1, June 2005, pp. 464–469.

[23] H. Urkowitz, "Energy detection of unknown deterministic signals," *Proc. IEEE*, vol. 55, no. 4, pp. 523–531, April 1967.

[24] A. N. Mody, *Spectrum Sensing of the DTV in the Vicinity of the Video Carrier Using Higher Order Statistics*, IEEE Std. 802.22-07/0359r0, July 2007.

[25] *Initial signal processing of captured DTV signals for evaluation of detection algorithms*, IEEE Std. 802.22-06/0158r2, August 2006.

[26] C. L. Nikias and A. P. Petropulu, *Higher-Order Spectra Analysis*. New Jersey: Prentice-Hall, 1993.

[27] (2010) Wikipedia webpage on Rayleigh distribution. [Online]. Available: http://en.wikipedia.org/wiki/Rayleigh-distribution

[28] A. Renaux, P. Forster, P. Larzabal, and E. Boyer, "Unconditional maximum likelihood performance at finite number of samples and high signal-to-noise ratio," *IEEE Trans. Signal Process.*, vol. 55, no. 5, pp. 2258–2364, May 2007.

[29] N. Menemenlis and C. D. Charalambous, "An Edgeworth series expansion for multipath fading channel densities," in *Proc. IEEE Conference on Decision and Control*, vol. 4, December 2002, pp. 4030–4035.

[30] H. Cramer, *Random Variables and Probability Distributions*. Cambridge University Press, 1970.

[31] L. Lu, K. Yan, and H.-C. Wu, "Novel robust gaussianity test for sparse data," in *Proc. IEEE International Conference on Acoustics, Speech and Signal Processing*, March 2010.

[32] C. Clanton, M. Kenkel, and Y. Tang, *Wireless microphone signal simulation method*, IEEE Std. 802.22-07/0124r0, March 2007.

[33] S. Shellhammer, *Numerical Spectrum Sensing Requirements*, IEEE Std. 802.22-06/0088r0, June 2006.

[34] S. Shellhammer, V. Tawil, G. Chouinard, M. Muterspaugh, and M. Ghosh, *Spectrum Sensing Simulation Model*, IEEE Std. 802.22-06/0088r0, March 2006.

Lu Lu received the B.S.E.E. degree from Taiyuan University of Science and Technology, Taiyuan, Shanxi, China, P.R.O.C. in 2005. He received the M.S. degree from Xian Jiaotong University, Shaanxi, China, P.R.O.C. in 2008. He is currently working toward the Ph.D. degree in electrical and computer engineering, Louisiana State University, Baton Rouge, Louisiana, USA. His research interests are in the area of digital communication, digital signal processing, and statistical signal processing.

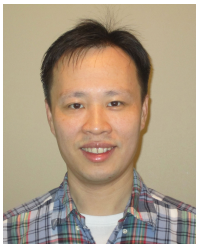

Hsiao-Chun Wu (M'00-SM'05) received a B. S. E. E. degree from National Cheng Kung University, Taiwan, in 1990, and the M. S. and Ph. D. degrees in electrical and computer engineering from University of Florida, Gainesville, in 1993 and 1999 respectively. From March 1999 to January 2001, he had worked for Motorola Personal Communications Sector Research Labs as a Senior Electrical Engineer. Since January 2001, he has joined the faculty in Department of Electrical and Computer Engineering, Louisiana State University, Baton Rouge, Louisiana, USA. From July to August 2007, Dr. Wu had been a visiting assistant professor at Television and Networks Transmission Group, Communications Research Centre, Ottawa, Canada. From August to December 2008, he was a visiting associate professor at Department of Electrical Engineering, Stanford University, California, USA.

Dr. Wu has published more than 140 peer-refereed technical journal and conference articles in electrical and computer engineering. His research interests include the areas of wireless communications and signal processing. Dr. Wu is an IEEE Senior Member and an IEEE Distinguished Lecturer. He currently serves as an Associate Editor for IEEE Transactions on Broadcasting, IEEE Signal Processing Letters, IEEE Communications Magazine, International Journal of Computers and Electrical Engineering, Journal of Information Processing Systems, Physical Communication, Journal of the Franklin Institute, and International Journal of Advancements in Technology. He was a Lead Guest Editor for IEEE Journal of Selected Topics in Signal Processing and Journal of Communications. He used to serve as an Associate Editor for IEEE Transactions on Vehicular Technology. He has also served for numerous textbooks, IEEE/ACM conferences and journals as the technical committee, symposium chair, track chair, or the reviewer in signal processing, communications, circuits and computers.

S. S. Iyengar (F'95) is the Roy Paul Daniels Chaired Professor and Chairman of Computer Science at Louisiana State University, and he is also been the Chaired Professor at various institutions(Satish-Dhawan Professorship, Homi-Bhaba Professorship, Jawaharlal Nehru Professorship, Asian University Professorship-Taiwan and Visiting professor in University of Paris and University of Bonne etc) around the world. He has been a visiting professor/scientist at Jet Propulsion Lab, Oakridge National Laboratory etc. His research interests include high-performance algorithms, data structures, sensor fusion, data mining, and Computational aspects of intelligent systems. He has co-authored 8 books (published by John Wiley, Prentice Hall, CRC Press, Springer- Verlag and etc) and edited 7 books published by IEEE Press and others. He has published over 380 research papers. He is a SIAM Distinguished lecturer/ ACM National Lecturer/ IEEE Distinguished Scientist. He is a Fellow of IEEE, Fellow of ACM, Fellow of AAAS and Fellow of SDPS (Society for Design and Process Science), Member of the European Academy of Sciences. He is a recipient of various IEEE awards, best paper awards, the Distinguished Alumnus award of the Indian Institute of Science, Bangalore and other awards.

He has served as the editor of several IEEE journals and is the founding editor-in-chief of the International Journal of Distributed Sensor Networks. His research has been funded by National Science Foundation (NSF), Defense Advanced Research Projects Agency (DARPA), Multi-University Research Initiative (MURI Program), Office of Naval Research (ONR), Department of Energy/OakRidge national Laboratory (DOE/ORNL), Naval Research Laboratory (NRL), National Aeronautics and Space Administration (NASA), US Army Research Office (URO) and various state agencies and companies. He has won Distinguished Research Master Award/LSU Rain Makers Award/ Hub Cotton Award for faculty excellence.